TEST OF A MODEL COMPOSITE BEAM WITH A WEB OPENING

By

SANJAY N. GATTANI

B. Tech., Indian Institute of Technology, India, 1985

A MASTER'S THESIS

Submitted in partial fulfillment of the

requirements for the degree

MASTER OF SCIENCE

Department of Civil Engineering

KANSAS STATE UNIVERSITY
Manhattan, Kansas

1987

Approved by:

Peter B. Cooper
Major Professor

TABLE OF CONTENTS

TABLE OF CONTENTS (continued)

LIST OF TABLES

LIST OF FIGURES

LIST OF FIGURES (continued)

CHAPTER 1

INTRODUCTION

Composite construction is the predominant construction method for floor systems in multi-story buildings. Openings in the webs of steel floor beams in a building are frequently used to permit the passage of pipes and conduits, thereby eliminating the need for space for these utilities beneath the beams. This can result in a sizeable reduction in steel requirements by decreasing building story height, thus achieving significant economy.

Recently, ultimate strength theories have been developed for composite beams with web openings; however, only a few tests have been conducted to check their adequacy. The successful development of a modeling technique for composite beams with web openings will make it possible to investigate with models a large range of parameters needed to validate theoretical predictions. This study was directed toward the development of methods of constructing model composite beams with web openings.

CHAPTER 2

REVIEW OF PREVIOUS WORK

2.1 Composite Beams with Web Openings

In the recent past, a number of investigators have developed ultimate strength analyses of composite beams with web openings.

Recently, Clawson and Darwin (2) have published the results of six ultimate load tests. Each of the six tests cited were on composite beams with concentric, unreinforced, rectangular openings. The opening depth in each case was about 0.6 times the steel beam depth. The opening length-to-depth ratio was 2 for all the tests. The ratio of moment-to-shear at the centerline of the opening varied from 2 ft. to 33 ft. The available ultimate strength theories provide reasonable, although somewhat conservative, estimates of the ultimate strengths of the six test beams.

2.2 Preliminary study of a Model Composite Beam with a Web Opening

As an undergraduate honors research project, Scully (4) fabricated and tested a model composite beam with a web opening at Kansas State University in 1981. A S4x9.5 steel beam was selected to model the prototype W18x45, because the model depth and flange area both provided a geometric scale factor of about 4.5. The web thickness in the vicinity of the opening was reduced by milling to maintain the same

scale factor. The slab dimensions were scaled down from the prototype, and the compressive strength of the model was similar to, although somewhat higher than, that of the prototype. Shear connectors were modeled with steel bolts tapped into the compression flange, and slab reinforcement was provided by threaded rods and longitudinal wires.

Because of the limited nature of this study, loads and deflections were the only data recorded. Also, due to an error in testing procedure, data were not obtained at ultimate load. However, based on a comparison of the load-deflection curves and failure mode of the model with those of the prototype tested by Clawson and Darwin (2), it was concluded that the behavior of the two members was similar.

2.3 Object and Scope

The prime objective of this study was to design and test a model composite beam in order to explore the possibilty of using model composite beams with web openings to generate test data. This test data was then compared with results obtained from a full-size, prototype beam.

This study was directed toward the development of methods of constructing model composite beams with web openings. Subsequent utilization of these methods will permit the investigation with models of the effect of key parameters in the ultimate strength predictions.

CHAPTER 3

MODELING

3.1 General

Similitude in modeling is needed in designing the model (geometry and materials), in establishing model loading intensities and time histories, and in predicting the results of the prototype structure from the measured model response.

Similitude relations are derived by establishing a complete set of pertinent dimensionless ratios from the various physical parameters involved in the particular study at hand, and then forcing these dimensionless ratios to be equal in model and prototype. Scaling laws come directly from the forced equalities. For a problem that has n parameters expressible in r different basic fundamental measures (dimensions such as length, time, force, temperature), it can be shown that there will be m=n-r dimensionless ratios and hence (n-r) scaling relationships to be enforced in the model study (3,5,7).

A model intended to portray behavior through the failure stage is known as a Static Strength model. Hence the models must be built from model concrete and small-scale reinforcement with properties similar to prototype materials. In fact, the failure criteria for model and prototype should be identical, but this is usually relaxed to the simpler requirements of similar stress-strain curves

for model and prototype in both uniaxial tension and compression.

3.2 Dimensional Analysis

The pertinent physical parameters are t_w, t_f, b_f, d, b_E, t_s, L, E_s, E_c, ϵ, σ_s, σ_c, P, M, V, ρ_s, ρ_c, b_s, δ. The parameters can be expressed in dimensions of force, F, and length, L, as shown in Table 3.1.

Since n=19 and r=2, there will be 17 dimensionless ratios and scaling factors to be enforced. A proper (but not unique) set of 17 dimensionless ratios is given by (3): t_w/L, t_f/L, b_f/L, d/L, t_s/L, E_s/E_c, σ_s/E_c, σ_c/E_c, P/E_cL^2, M/E_cL^3, V/E_cL^2, ρ_sL/E_c, ρ_cL/E_c, δ/L

The first scaling factor is determined by setting the ratios,

$$(t_w/L)_m = (t_w/L)_p$$

i.e. $$(t_w)_m = (t_w)_p(L_m/L_p)$$

where the subscripts m and p denote model and prototype, respectively. The ratio (i_p/i_m) will be defined as the scale, S_i, for quantity i.

Similitude requirements for the model are given in Table 3.1. $S_\sigma = S_E = 1$, or model and prototype materials have identical strengths, failure strains, and modulii.

CHAPTER 4

EXPERIMENTAL INVESTIGATION

4.1 General

The prototype for the model beam is Beam No. 5 tested by Clawson and Darwin at the University of Kansas (2). The prototype test specimen was an A36 steel, W18x46 steel beam with a 4in. x 48in. concrete slab having a compressive strength of 4680 psi. The opening, 10-13/16" x 21-5/8", was concentric and rectangular with a moment-shear ratio of 6 ft. at the centerline of the opening. Mechanical connection between the steel beam and concrete slab was provided by standard 3/4" diameter studs, 3" long (see Fig. 4.1).

Extensive testing of all the model materials was conducted and is discussed later in Chapter 5.

4.2 Design of Model Beam

To construct a direct model, it is necessary that the stress-strain curves and the geometric properties of the model and the prototype be the same (3). The use of an A36 steel W8x10 steel beam to model the prototype beam met this criteria with a linear scale factor of 2.2. A comparison of the model beam section with the prototype section is given in Table 4.1.

Slab and opening dimensions were scaled directly from those of the prototype, and a micro-concrete mix was used that has stress-strain characteristics similar to the prototype. This mix has been extensively used in concrete

model studies at Kansas State University (6). The studs (3/8" x 1-3/8") were specially made by Nelson Stud Welding Division of TRW for this model. Threaded rods were used for reinforcement of the slab as shown in Fig. 4.2.

The opening location, load configuration and span length for the beam are shown in Fig. 4.3.

4.3 Beam Fabrication

The steel beam was cut to the desired length. The opening location was marked, and 3/8" diameter holes were drilled at the corners to reduce stress concentrations. The opening was then cut by milling. Strain gage locations were ground with an abrasive wheel. Bearing plates for the model beam supports were welded in place. Studs were welded using a Nelson Stud Welding Unit. The beam was then instrumented with strain gages.

The concrete formwork was constructed using plyform and 2"x2" steel angles milled to the modeled thickness of the concrete slab (see Fig. 4.7). Holes were drilled in the angles at 3-11/16" spacing to support 5/16" diameter threaded rods for transverse reinforcement. Supports were provided for the formwork at 2-1/2 foot intervals along the beam. All joints in the formwork were then sealed with silicone rubber gel, and the formwork was oiled. After the transverse reinforcing rods were placed in position, longitudinal reinforcement was tied below them. Splices in the longitudinal steel were designed in accordance with the

ACI Building Code (10), and were not placed in the vicinity of the opening.

Two batches of concrete were prepared. Standard sized test cylinders (3"x6") were cast as the beam was cast. More cylinders were cast for the batch of concrete that was poured over the web opening. After the concrete had begun to set, the slab and the test cylinders were covered with polyethylene sheets. The beam and the cylinders were kept moist during the early stages of curing. The formwork was removed and the concrete allowed to dry two days before the day of testing.

4.4 Instrumentation

The beam was instrumented with electrical strain gages placed on both the steel beam and the concrete in the vicinity of the opening. The gages were located at sections 0.68" from the vertical edges of the opening to reduce the effect of stress concentrations at the opening corners. Concrete gages were placed on the top and bottom of the slab. Three-gage rosettes were placed at the corners of the opening to measure shearing strains.

The strain gages on the steel beam were 120 ohm, 1/8" gage length foil gages and the concrete strain gages were 120 ohm, 3/8" gage length. Fig. 4.5 shows the locations of the gages on the beam. The gages were placed following the gage manufacturer's recommended procedure. All gages were wired with 3-wire shielded cables. The strain gages were

read using a Vishay 40-channel Data Acquisition System.

Vertical deflections of the beam were measured at several locations using dial gages graduated in 0.001" (see Fig. 4.8). The dial gages were place at a section 0.68" inside the vertical edges of the opening to measure the Low Moment Edge and the High Moment Edge deflection. As the ends of the base beam would deflect under the load, it was necessary to measure the base beam deflection at the model beam support points also. Dial gages were also used at the ends of the beam to measure relative displacements between the concrete and steel. These gages were graduated in 0.0001". Fig. 4.4 shows the locations of the dial gages.

Hydrated lime mixed with water (whitewash) was applied to the entire steel beam to provide visual information on the critical areas of yielding around the opening.

4.5 Load System

When the concrete reached the desired strength, the formwork was removed and the beam was simply supported on pin supports. Bearing plates were placed on the concrete slab at the load points (see Fig. 4.6). The beam was loaded at two points through a spreader beam using a Southwark-Emory 300,000lb hydraulic universal testing machine.

4.6 Loading Procedure

Before testing, the beam was cycled 3 times to load values of 1000 lbs. to check out the test set-up and the instrumentation. After these preliminary cycles, three

elastic tests and an ultimate strength test were conducted.

4.6.1 Elastic Test

All gages were zeroed before loading. The beam was loaded in small increments to a maximum load of 5 kips, well below the yield strength of the beam (first yield). After each load increment was applied, the strain gages and deflection gages were read. After the peak load was reached and data recorded, the beam was unloaded and data recorded at the same load intervals.

4.6.2 Ultimate Strength Test

Before starting the test, all gages were zeroed. Initially, constant load increments of 2 kips were applied. Load control was used until the relative displacement between the two edges of the opening became non-linear. From this point, deflection control was used with the centerline deflection of the beam being the controlled deformation.

Concrete cracks were marked with a felt-tip pen. Cracks were identified by indicating the load at which they formed. After the beam failed, the load was removed and additional cracks were marked. Photographs of the beam were taken towards the end of the test.

CHAPTER 5

MATERIALS

5.1 Concrete

Micro-concrete is the most suitable material for model concrete construction.

The components of the micro-concrete mix used in this investigation are Type I cement, Kaw River sand and water. This mix has been used on a number of modeling projects conducted at Kansas State University (6). The following table gives the quantities of the materials per cubic feet of concrete:

Material	Quantity
1. Type I cement	38.46 lb
2. Sand (passed through sieve #16)	76.92 lb
3. Water	19.23 lb

(Unit Weight = 134.61 lb/cu.ft.)

The compressive strength of concrete used in the prototype was 4680 psi on the day of test. A preliminary batch of model concrete was prepared in an attempt to obtain the strength vs. age of concrete curve. Twenty-one standard size cylinders were cast and cured by keeping them moist in the open air. The cylinders were tested regularly and the strength vs. age of model concrete curve was plotted (see

Fig. 5.1). The concrete was thus estimated to attain the desired strength within about 18 days.

Twenty-six 3"x6" cylinders were cast according to ASTM standards along with the test beam. The cylinders were covered with a polyethylene sheet, in a manner similar to the test beam, throughout the curing stage and were kept moist continuously. These cylinders were periodically tested to monitor the concrete strength. Because of scheduling difficulties and a more rapid development of compressive strength in the concrete than anticipated, the actual compressive strength of concrete was found to be 5375 psi when the model composite beam was tested. One cylinder was instrumented with strain gages to obtain the stress-strain data.

Table 5.1 show the test results for the cylinders of the two batches of concrete used for the test beam.

Fig. 5.2 show the compressive stress-strain curve for the micro-concrete tested at 11 days.

5.2 Structural Steel

The steel section used in the model beam was a hot rolled, A36 W-shape beam. Tensile tests were conducted on coupons cut from the beam. Two longitudinal coupons were cut from each of the flanges and three were cut from the web. The coupons were machined to standard 10" ASTM tensile coupons.

Tensile tests were conducted on a screw-type testing

machine. The cross-sectional dimensions were measured using a micrometer graduated in 0.001". The coupons were fitted with an extensometer to obtain load-deflection plots during the test. The yield strength, static yield strength and tensile strength of the material were measured during each test. Specimens were loaded through the yield plateau at a crosshead speed of 0.25mm/min. After the steel began to yield, the displacement was stopped. The load would drop and stabilize (at the static yield load) within about 10 minutes. Loading was resumed, and then stopped again to obtain a second static yield load. The loading was then continued until the coupons reached the ultimate tensile strength. The results of a typical test are presented in Fig. 5.3. Table 5.2 lists the steel properties for all the test coupons.

5.3 Reinforcing Steel

Threaded rods were used to reinforce the concrete slab. The longitudinal and transverse reinforcement consisted of 8-32 diameter rods and 5/16" diameter rods, respectively. The reinforcing rods were tested for yield strength and tensile strength. The yield stress of the rods was measured using the 0.2% offset method. Material strengths of the reinforcing are shown in Table 5.2.

5.4 Shear Studs

A pushout test of the studs was conducted to determine the behavior and load carrying capacity of stud shear

connectors.

5.4.1 Details of Pushout Specimen

The pushout specimen was a double slab specimen on a W8x10 steel section. The size of the specimen was scaled down from the standard pushout specimen as recommended by Ollgaard of Lehigh University (11). The specimen is shown in Fig. 5.4. The slab dimensions are txbxh = 1.82"x6.07"x11.28" with four studs (d x h = 3/8" x 1-3/8") in each slab. The reinforcement in each slab consisted of four vertical loops of 5/16" diameter threaded rods and four horizontal loops of 8-32 threaded rods.

5.4.2 Fabrication Procedure

The reinforcing rods were tied together to form a 2-layer mesh. The pushout specimen was cast in the same position in which it was to be tested. 21 cylinders (3"x6") were cast along with the specimen. The specimen and the test cylinders were covered with a polyethylene sheet and kept moist during curing stages. The cylinders were periodically tested to monitor the strength of the concrete. The formwork was removed and concrete allowed to dry two days before the day of testing.

5.4.3 Test of Pushout Specimen

The specimen was centered in the testing machine with the lower ends of the slabs bedded in cylinder capping compound to provide uniform bearing. The load was applied to the upper end of the steel beam through a steel bearing plate (see Fig. 5.5). The movement of the machine head,

measured with 0.001" dial indicators, represented the slip between the slabs and the steel section. The results of the pushout test are illustrated in Fig. 5.6 and Fig. 5.7.

5.4.4 Tensile Test on Studs

Three welded studs were tested in tension to find the tensile strength of the studs and to check the adequacy of the weld strength. A special assembly, shown in Fig. 5.8, was prepared to apply tension to the studs. The assembly consisted of two components; one to which the stud was welded and the other to hold the head of the stud in position. The studs were found to have an average ultimate tensile strength of 61 ksi.

CHAPTER 6

EXPERIMENTAL RESULTS

6.1 General

The deformation and the failure mode of composite beams with web openings is largely a function of the moment-shear ratio at the opening (1). For openings with low M/V ratios, the Vierendeel effect becomes pronounced, as the shear at the opening induces secondary bending moments in the web. The openings tend to have large differential deflections and beams with solid slabs tend to display a diagonal tension failure in the slab (1).

6.2 Test Results

Three elastic tests and one ultimate strength test were conducted on the model composite beam. One elastic test was selected for the purpose of presentation and evaluation. Load-slip diagrams for the elastic tests are not presented due to the negligible values recorded.

Large differential deformation across the opening was observed as the beam was loaded (see Fig. 6.2). The maximum beam deflection was found at the centerline of the test beam. The deflection at the high moment end of the opening had the next greatest deflection followed by the deflection at the low moment end of the opening. The load-deflection curves are shown in Fig. 6.3 and Fig. 6.4. The strain readings (see Fig. 6.8-6.9) show the effect of the moment-shear ratio.

The strain distributions at the end of the top and bottom tees are illustrated in Fig. 6.10. The presence of compressive as well as tensile strains in the bottom tee indicates the presence of Vierendeel action.

The model composite beam failed by excessive deflection of the beam at the high moment edge of the opening relative to the deflection at the low moment edge of the opening. The peak load was preceeded by major cracking in the concrete slab, yielding of the steel, and large deflections in the beam.

6.3 Behavior under Load

As the test beam had a low moment-shear ratio (M/V = 2.73 ft.), the behavior under load was dominated by secondary bending moments. At elastic loads (Fig. 6.10), the low moment end of the bottom tee was in tension, while a compressive zone was present in the top of the web at the high moment end. First yielding was observed in tension, and it occured at the low moment end of the bottom tee. Small compressive strains were present at the low moment end of the bottom tee, as the beam approached the ultimate load. The remainder of the low moment end yielded in tension. The high moment end of the bottom tee yielded in compression at the top of the web and yielded in tension in the flanges and in the remainder of the web. In the top tee, the steel yielded in tension at the high moment end and in compression at the low moment end. As the test progressed, the steel

and concrete began to separate near the center of the opening. The load-slip curve for the ultimate strength test is presented in Fig. 6.5. A large, diagonal, tension crack formed at this point, and began propagating outward on the bottom of the slab towards the high moment end of the opening. Simultaneously, a transverse crack formed in the top of the slab at the low moment edge of the opening.

At about 90% of the ultimate load, a large separation occurred between the steel and the concrete over the centerline of the opening. All transverse, diagonal and longitudinal cracks were noted in the slab as the load increased. At the ultimate load, the diagonal cracks extended to the edge and propagated diagonally to the top of the slab towards the load point (see Fig. 6.11).

At all stages of loading, strains at the opening indicate a lack of strain compatibility between the top tee steel and the slab (Fig. 6.10). The strain data show that strains were quite low in the concrete slab at failure (Fig. 6.8). The ultimate load was recorded as 9.73 kips per load point. Fig. 6.9 shows the shearing strains obtained from the rosettes on the webs of the four tees. The results indicate that the shearing strains reversed trend when yielding began only to reverse again at higher loads.

6.4 Comparison of the Results with the Prototype Beam

Three different sets of results can be evaluated to determine if model composite beams with web openings can be

used to generate test data that accurately predict results obtained in testing full size composite beams with web openings. These are load vs. deflection & load vs. strain curves, mode of failure and the ultimate load carrying capacity of the beam.

The load vs. deflection and load vs. strain curves for the model beam are very similar to the curves plotted for the prototype beam. Moreover, the deflections at the ultimate load for the model beam compare very closely with the corresponding deflections for the prototype beam using a model scale factor of 2.2. The data acquisition system that was used to record the strains did not record strains greater than 3000 micro-in/in, due to which, the strain distribution in the test beam at loads near the failure load is not available. Hence, there is no basis to compare the strains in the model beam with that in the prototype at ultimate load. However, up to a load of 15-16 kips, the model beam had strains lower in magnitude than those in the prototype beam.

The failure of the model beam was a shear-type failure which was very similar to the mode of failure of the prototype.

The ultimate load for the model beam was 19.45 kips. Although this was about 8% higher than the expected value of 18 kips ($=87.1/2.2^2$), it compares favorably with the ultimate load for the prototype beam (87.1 kips).

CHAPTER 7

SUMMARY AND CONCLUSIONS

7.1 Summary

The purpose of this investigation was to explore the possibilities of modeling composite beams with web openings. One model beam was constructed and tested to failure. The experimental results were then compared with the results obtained in testing the prototype beam.

7.2 Conclusions

Based on the experimental results, it can tentatively be concluded that the behavior of the two members was similar, and that the prototype beam was quite accurately modeled.

7.3 Recommendations for Further Study

Only one model beam was tested in this project. Testing of an additional one or two model beams would be helpful in corroborating the conclusions of this study.

ACKNOWLEDGEMENTS

The author wishes to express his deep and sincere thanks to Dr. P. B. Cooper, for his kind guidance in carrying out this project. The author is deeply grateful to him for the keen interest he took at every stage of this work, and for the encouragement he provided without which this work would not have been a success. Dr. P. B. Cooper was a constant source of inspiration and acted as a friend, guide and philosopher.

The author also wishes to recognize the Nelson Stud Welding Division of TRW for supplying the stud welding equipment and the shear studs.

A debt of gratitude is owed to Mr. Russell Gillespie and to those friends who were always available to help.

REFERENCES

1. Clawson, W. C. and Darwin, D., "Strength of Composite Beams with Web Openings," Journal of the Structural Division, ASCE, Vol. 108, No. ST3, March 1982.

2. Clawson, W. C. and Darwin, D., "Tests of Composite Beam with Web Openings," Journal of the Structural Division, ASCE, Vol. 108, No. ST1, Jan. 1982.

3. Kong, F. K., Evans, R. H., Edward Cohen and Fredric Roll, "Handbook of Structural Concrete," McGraw Hill, 1983.

4. Scully, M. J., "Model Composite Beams with Web Openings," Undergraduate Honors Research Paper, Dept. of Civil Engineering, Kansas State University, March 1981.

5. Sabnis, G. M., Harris, H. G., White, R. N. and Mirza, M. S., "Structural Model and Experimental Techniques," Prentice Hall, Inc., 1983.

6. Zregh, A. S., "Local Instability Behavior and Collapse of a Long Span Concrete Folded Plate Model," Ph.D. Dissertation, Dept. of Civil Engineering, Kansas State University, 1984.

7. ACI Publication No. 24, "Models for Concrete Structures," American Concrete Institute, 1970.

8. Viest, I. M., "Investigation os Stud Shear Connectors for Composite Concrete and Steel T-Beams," Journal of the American Concrete Institute, Vol. 27, No. 8, April 1956.

9. ASTM, 1979 Annual Book of ASTM Standards, American Society for Testing and Materials, Philadelphia, Pa., Vol. 14.

10. ACI, Building Code Requirements for Reinforced Concrete (ACI 318-77), American Concrete Institute, Detroit, Michigan, 1977.

11. Ollgaard, J. G., Slutter, R. G., Fisher, J. W., "Shear Strength of Stud Connectors in Lightweight and Normal-Weight Concrete," Engineering Journal, American Institute of Steel Construction, Vol. 8, No. 2, April 1971.

Table 3.1

Dimensions of Parameters

Parameter	Dimensions	Scale Factor
1. Geometry:		
Linear dimension, L	L	S_L
Area, A	L^2	S_L^2
Moment of Inertia, I	L^4	S_L^4
Linear displacement, δ	L	S_L
2. Materials and related Parameters:		
Stress, σ	FL^{-2}	$S_E = 1$
Modulus of Elasticity, E	FL^{-2}	$S_E = 1$
Poisson's ratio, ν	---	1
Density, ρ	FL^{-3}	$S_E/S_L = 1/S_L$
Strain, ϵ	---	1
3. Loading:		
Concentrated force, P and Shear force, V	F	$S_E S_L^2 = S_L^2$
Pressure or uniformly distributed load, q	FL^{-2}	$S_E = 1$
Line load, w	FL^{-1}	$S_E S_L = S_L$
Moment, M	FL	$S_E S_L^3 = S_L^3$
Moment-Shear ratio, M/V	L	S_L

Table 4.1

Comparison of Model Beam with Prototype Beam

Section Properties	W18x46	W8x10	Scale Factor
1. Non-Composite:			
Area, A, in^2	13.5	2.96	$4.56 = (2.14)^2$
d, in	18.0	7.89	2.28
I, in^4	712	30.8	$23.12 = (2.19)^4$
t_f, in	0.605	0.205	2.95
b_f, in	6.0	3.94	1.523
A_f, in^2	3.63	0.807	$4.49 = (2.12)^2$
t_w, in	0.36	0.17	2.12
2. Composite:			
Area, A, in^2	39.34	8.305	$4.74 = (2.18)^2$
d, in	22.0	9.71	2.26
I, in^4	1800	77.15	$23.33 = (2.2)^2$

Table 5.1

Compressive Strength of Concrete

Cylinder No.	Age of Concrete	Load	Stress	Average Stress
	days	lbs	psi	psi
I. Batch 1:				
11	7	32000	4527	4372
21		29800	4216	
12	10	33400	4725	
22		38800	5489	5248
32		39100	5532	
13	11	36400	5150	
23		40000	5659	
33		36400	5150	5376
43		38200	5404	
53		39000	5517	
14	13	38800	5489	
24		37400	5291	5342
34		39800	5631	
44		35100	4956	

Table 5.1 (continued)

Compressive Strength of Concrete

Cylinder No.	Age of Concrete	Load	Stress	Average Stress
	days	lbs	psi	psi
II. Batch 2:				
11	11	41200	5829	
21		38500	5447	5712
31		42800	6055	
41		39000	5517	

Table 5.2

Steel Properties

Specimen	Yield ksi	Static Yield ksi	Tensile ksi
Flange No. 1	46.78	41.91	61.29
Flange No. 2	46.30	43.03	61.10
Web No. 1	55.77	52.41	66.90
Web No. 2	48.23	44.08	62.08
Reinforcement:			
a. 5/16"-18	84.13	-----	92.69
b. 8-32	90.71	-----	97.14

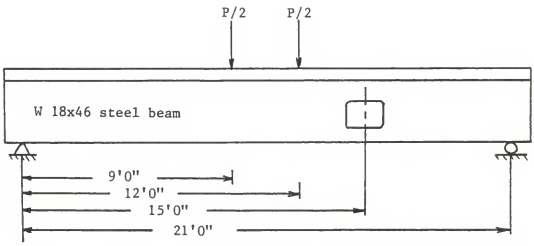

ELEVATION

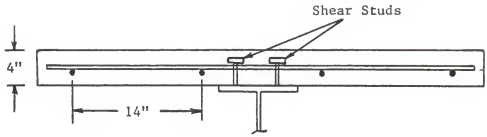

SIDE VIEW

Fig. 4.1 Details of the Prototype Beam

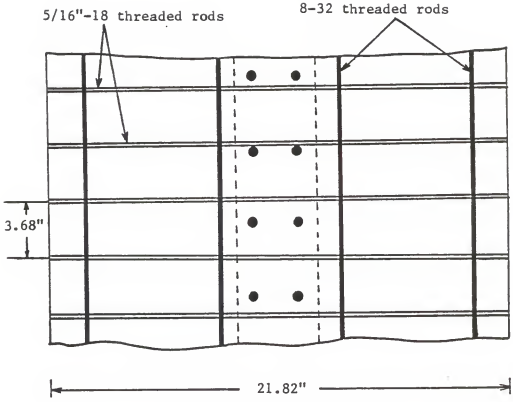

Plan View

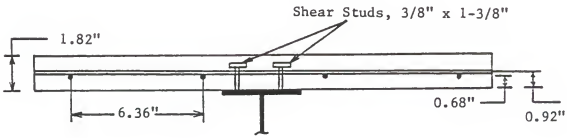

Side View

Fig. 4.2 Reinforcing Steel for the Model Beam

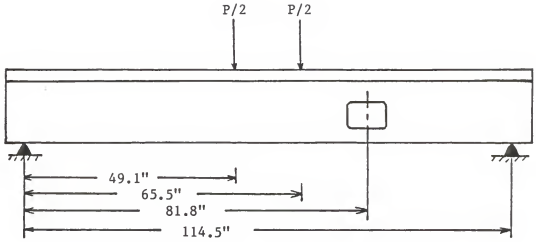

Fig. 4.3 Layout for the Model Beam

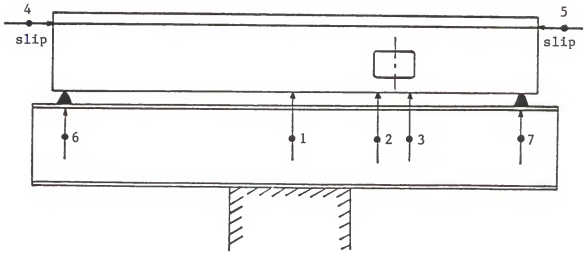

Fig. 4.4 Deflection Gage Locations for the Model Beam

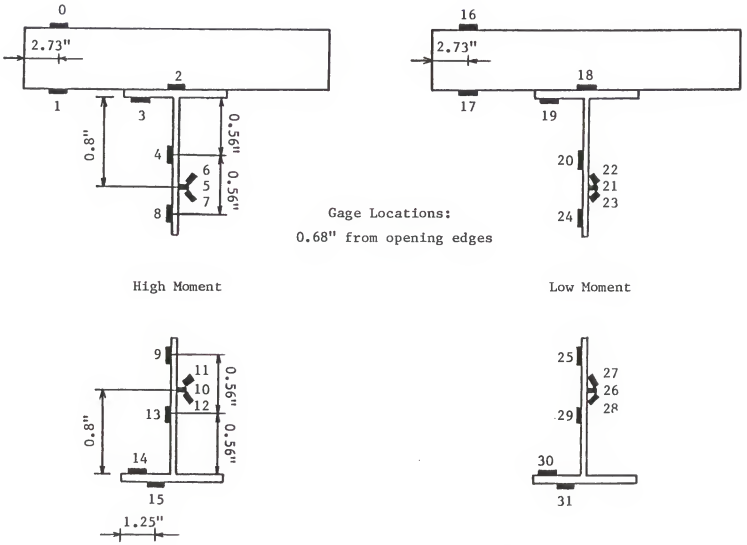

Fig. 4.5 Strain Gage Locations for the Model Beam

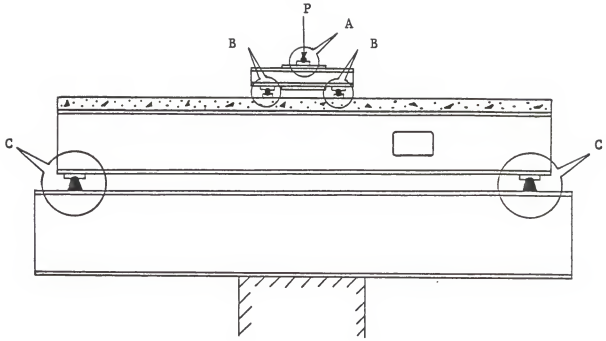

Detail A

Detail B

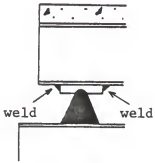

Detail C

Fig. 4.6 Schematic Test Set-up for the Model Beam

Fig. 4.7 Formwork for the Model Beam Slab

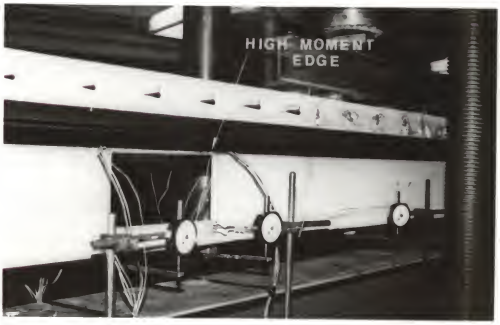

Fig. 4.8 Deflection Gage Locations for Model Beam

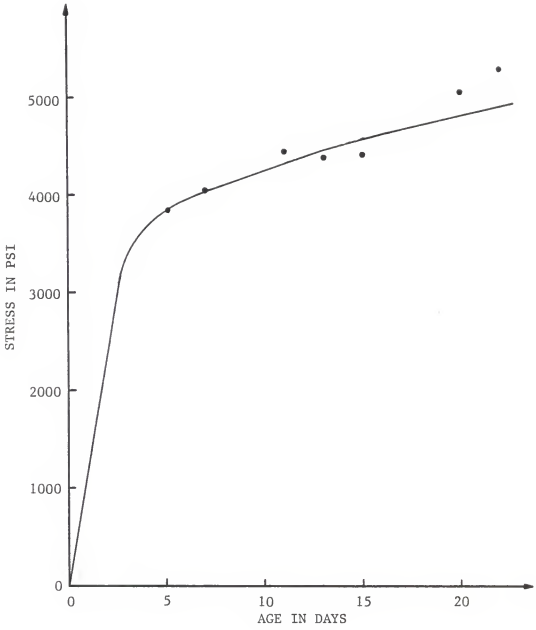

Fig. 5.1 Strength vs. Age Curve for Preliminary Batch of Concrete

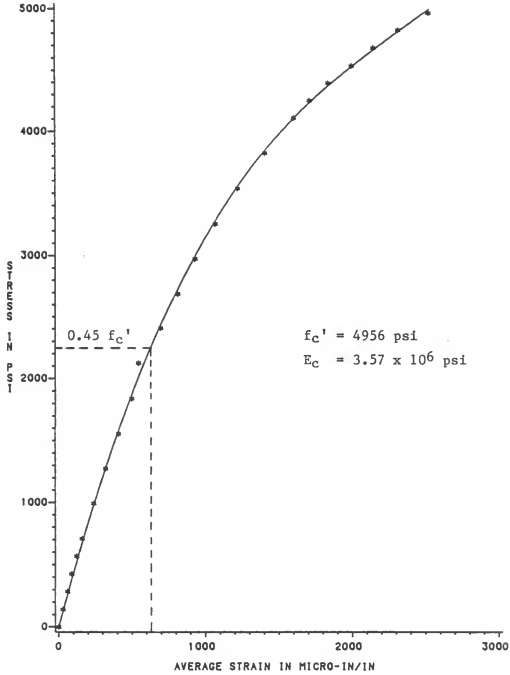

Fig. 5.2 Stress-Strain Curve for Model Concrete

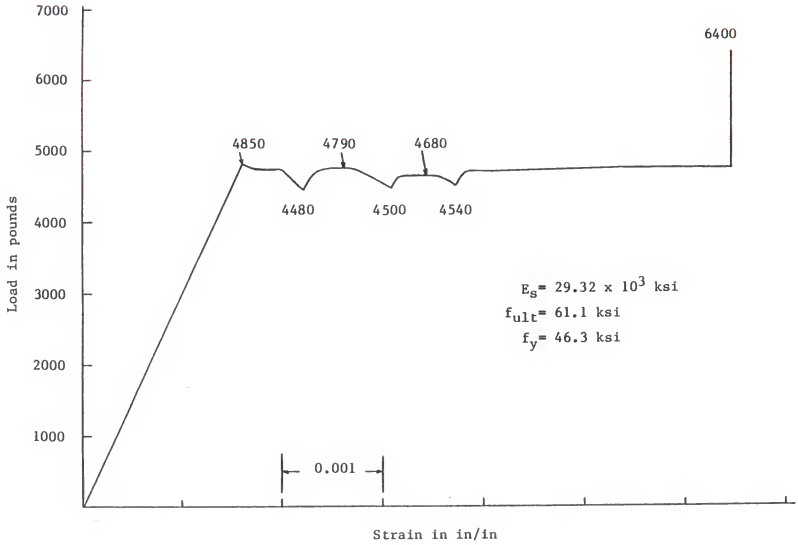

Fig. 5.3 Typical Load-Strain Curve for Structural Steel

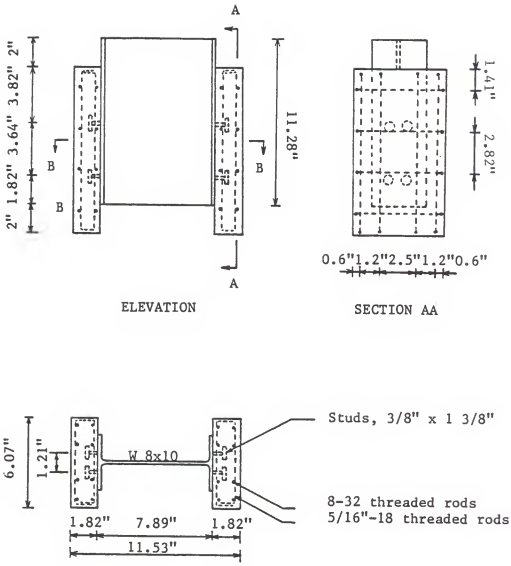

Fig. 5.4 Details of Pushout Specimen

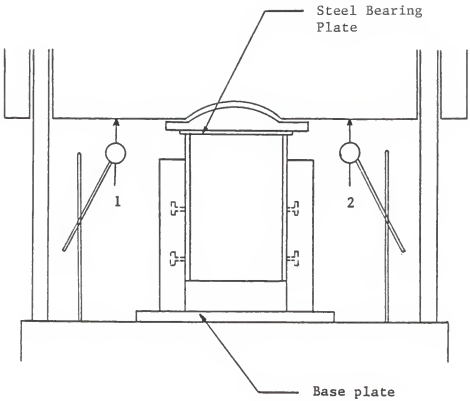

Fig. 5.5 Schematic Set-up for Pushout Test

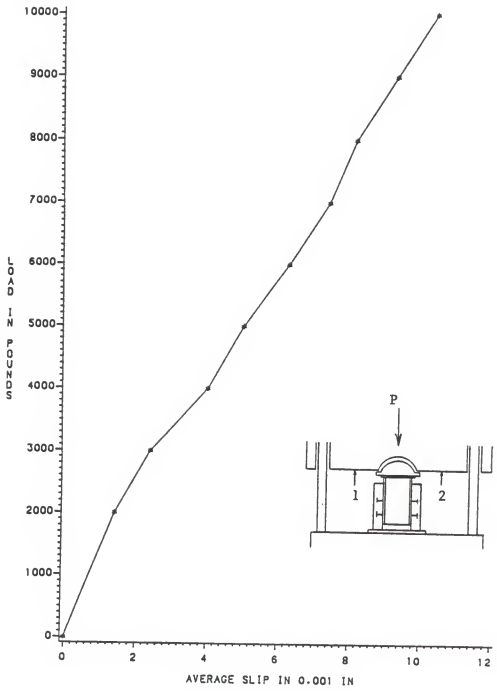

Fig. 5.6 Elastic Load-Slip Curve for Pushout Specimen

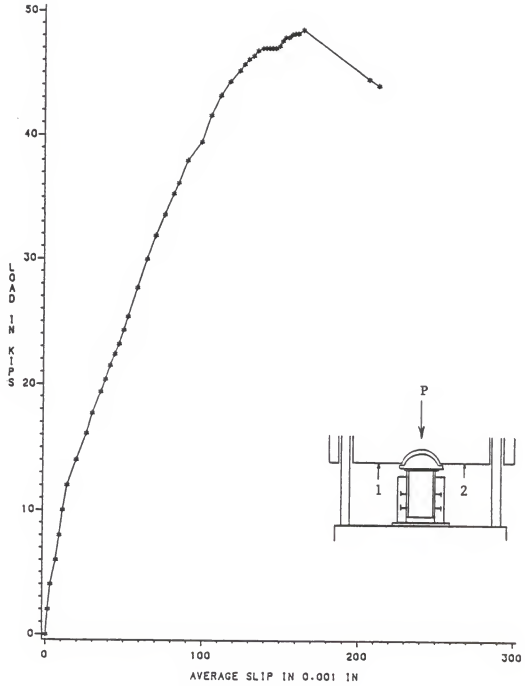

Fig. 5.7 Ultimate Load-Slip Curve for Pushout Specimen

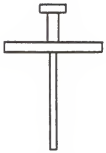

ELEVATION

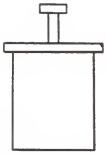

SIDE VIEW

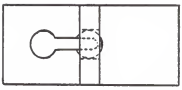

TOP VIEW

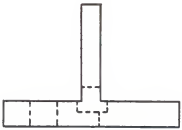

ELEVATION

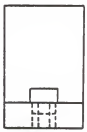

SIDE VIEW

Fig. 5.8 Assembly for Tension Test on Studs

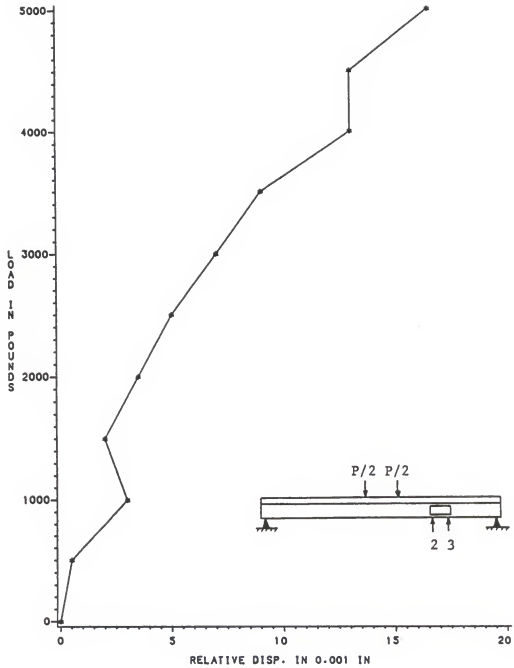

Fig. 6.1 Elastic Load-Relative Displacement Curve for Model Beam

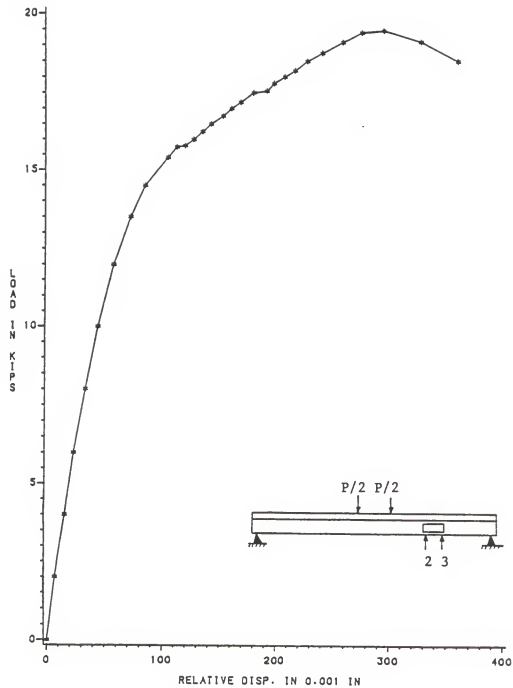

Fig. 6.2 Ultimate Load-Relative Displacement Curve for Model Beam

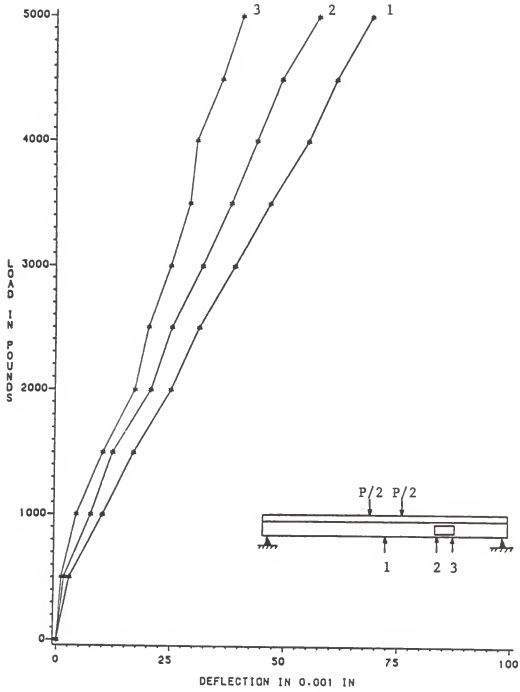

Fig. 6.3 Elastic Load-Deflection Curves for Model Beam

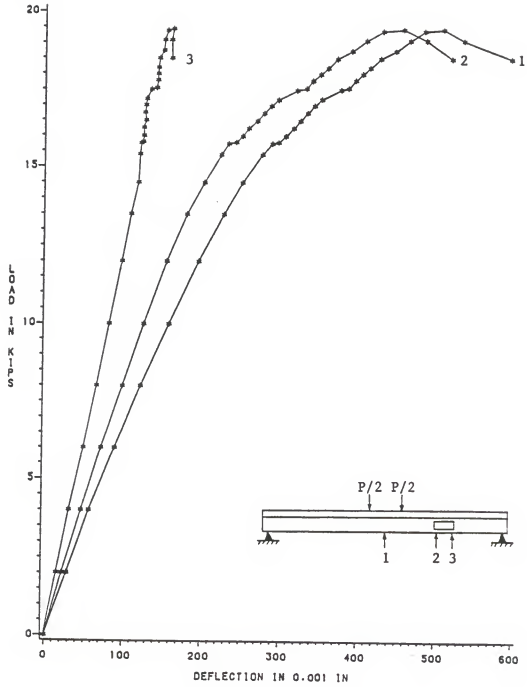

Fig. 6.4 Ultimate Load-Deflection Curves for Model Beam

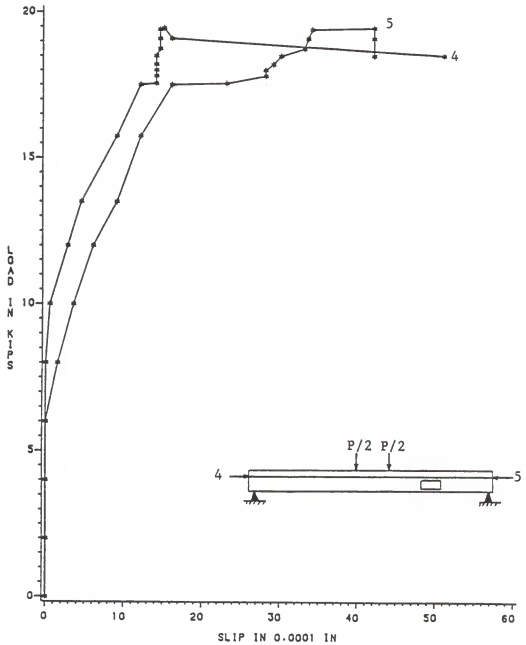

Fig. 6.5 Ultimate Load-Slip Curves for Model Beam

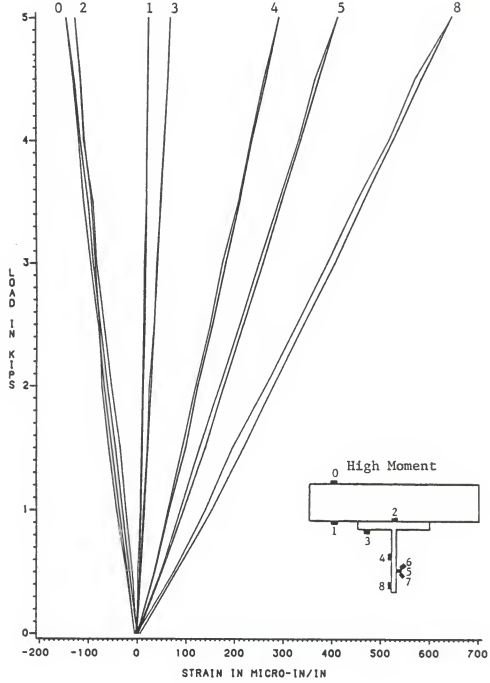

Fig. 6.6 Elastic Load-Strain Curves for Model Beam

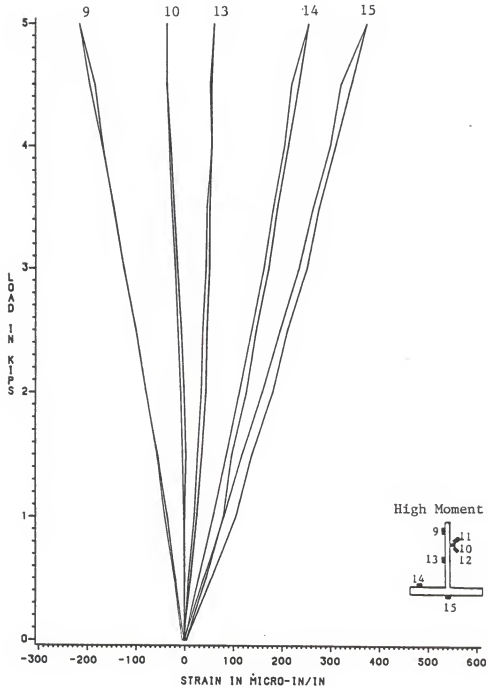

Fig. 6.6 Elastic Load-Strain Curves for Model Beam (contd.)

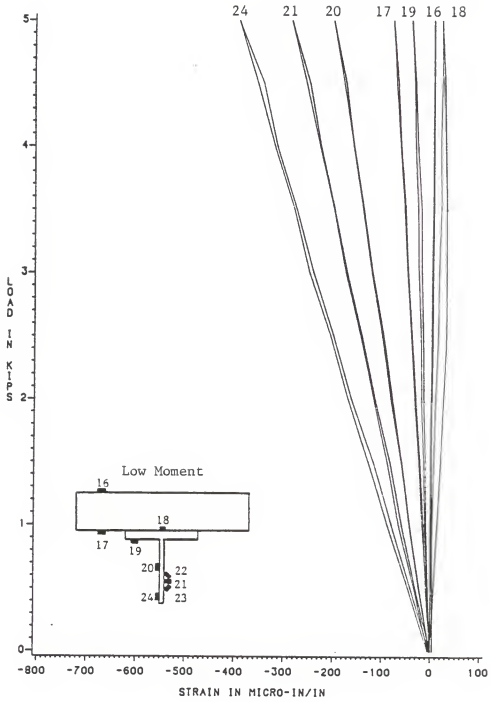

Fig. 6.6 Elastic Load-Strain Curves for Model Beam (contd.)

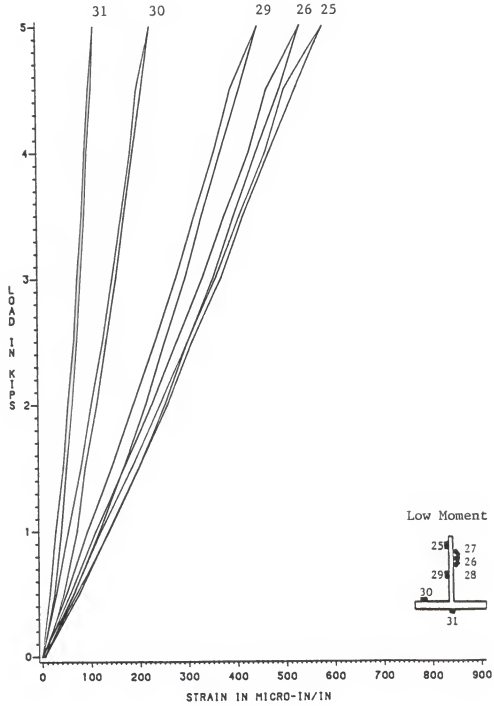

Fig. 6.6 Elastic Load-Strain Curves for Model Beam (contd.)

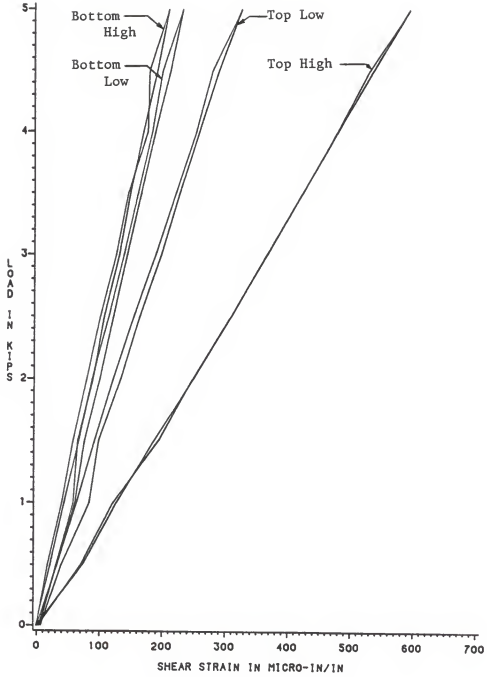

Fig. 6.7 Elastic Load-Shearing Strain Curves for Model Beam

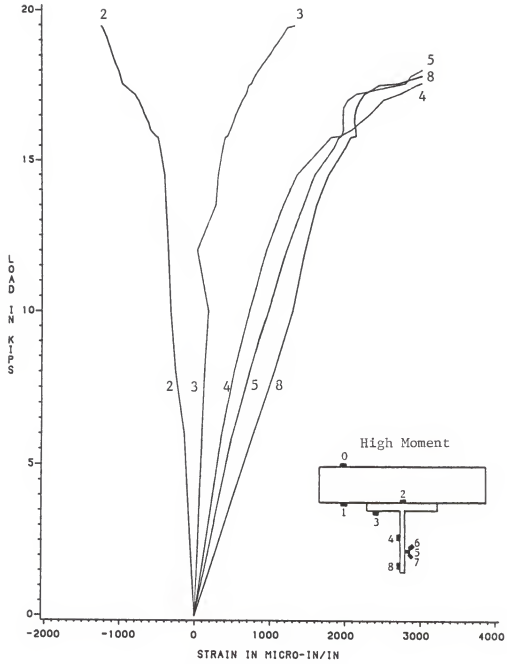

Fig. 6.8 Ultimate Load-Strain Curves for Model Beam

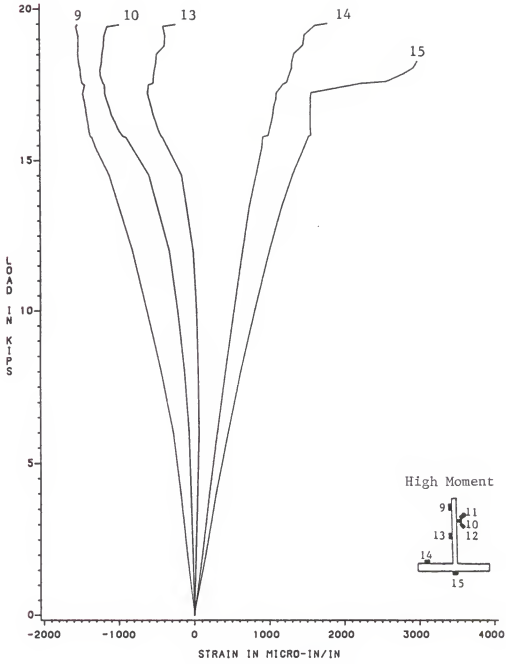

Fig. 6.8 Ultimate Load-Strain Curves for Model Beam (contd.)

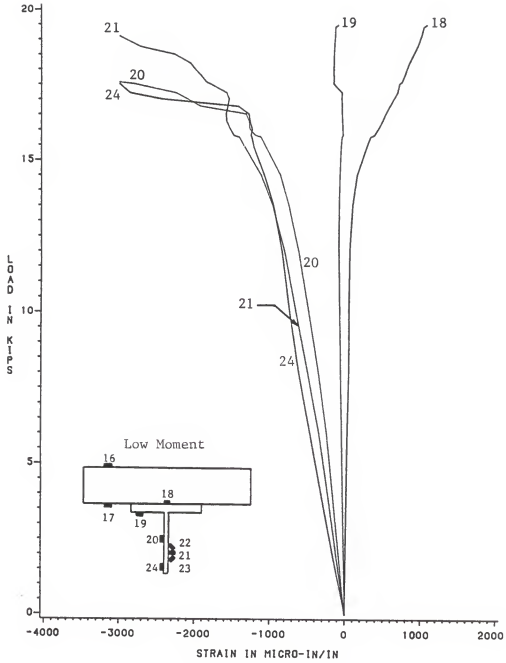

Fig. 6.8 Ultimate Load-Strain Curves for Model Beam (contd.)

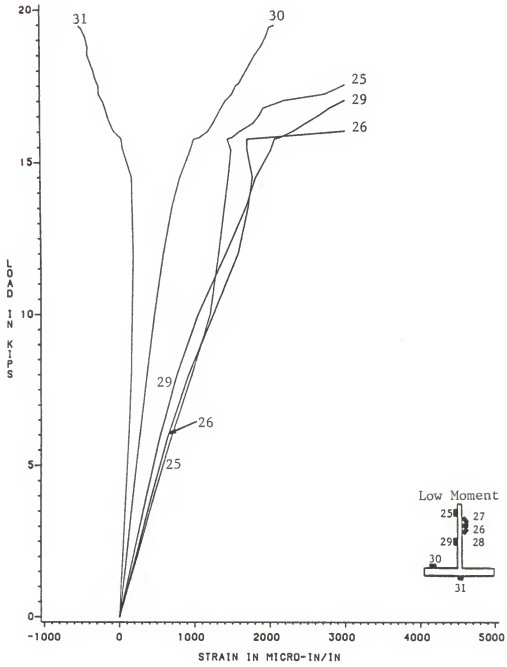

Fig. 6.8 Ultimate Load-Strain Curves for Model Beam (contd.)

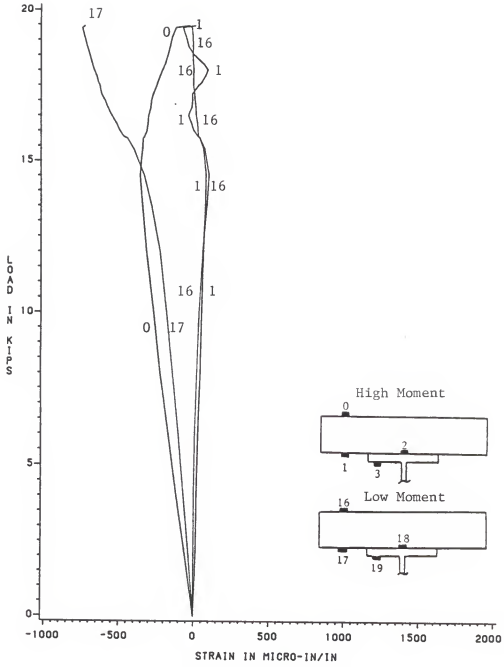

Fig. 6.8 Ultimate Load-Strain Curves for Model Beam (contd.)

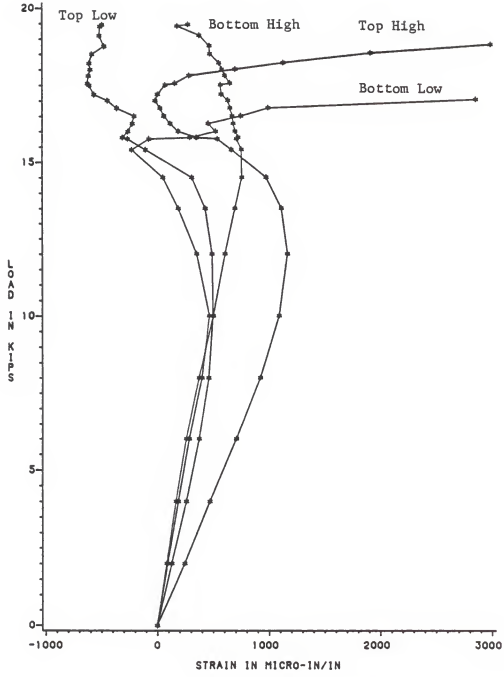

Fig. 6.9 Ultimate Load-Shearing Strain Curves for Model Beam

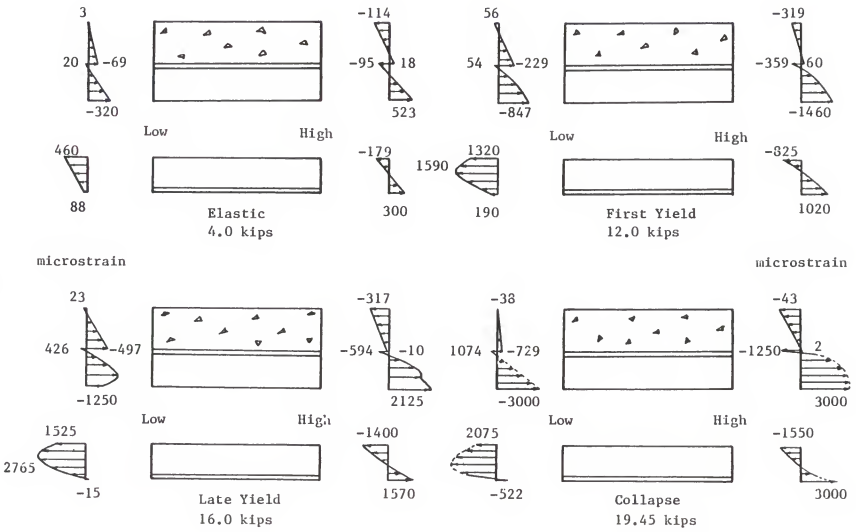

Fig. 6.10 Strain Distribution in Model Beam

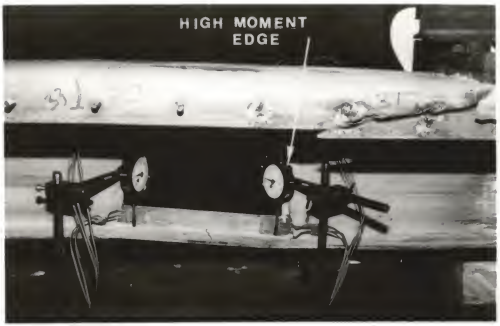

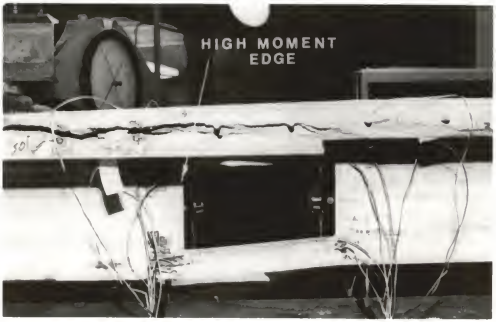

Fig. 5.11 Crack Pattern in Model Beam Slab

TEST OF A MODEL COMPOSITE BEAM WITH A WEB OPENING

By

SANJAY N. GATTANI

B. Tech., Indian Institute of Technology, India, 1985

AN ABSTRACT OF A MASTER'S THESIS

Submitted in partial fulfillment of the

requirements for the degree

MASTER OF SCIENCE

Department of Civil Engineering

KANSAS STATE UNIVERSITY
Manhattan, Kansas

1987

ABSTRACT

The purpose of this investigation was to develop methods of constructing model composite beams with web openings. One model composite beam with a geometric scale factor of 2.2 was built and tested to failure. The prototype test specimen had a moment-shear ratio at the centerline of the opening of 6 ft. This is in the medium range which is of particular interest in investigating the shear contribution of the slab. The test results were compared with those of the prototype to check the adequacy of the modeling techniques.

The most important test observations were the load-deformation response of the model, the ultimate load and the mode of failure. The peak load was preceeded by major cracking in the concrete slab, yielding of the steel and large deflections in the beam. The ultimate failure of the model beam was a shear-type failure due to large relative displacement between the ends of the opening.